JPNT 11(1), 11-21 (2022)
https://doi.org/10.11003/JPNT.2022.11.1.11

JPNT Journal of Positioning, Navigation, and Timing

Low Computational FFT-based Fine Acquisition Technique for BOC Signals

Jeong-Hoon Kim[1], Binhee Kim[2], Seung-Hyun Kong[1†]

[1]The CCS Graduate School of Green Transportation, Korea Advanced Institute of Science and Technology, Daejeon 34051, Korea
[2]Korea Aerospace Industries, Gyeongsangnam-do 52529, Korea

ABSTRACT

Fast Fourier transform (FFT)-based parallel acquisition techniques with reduced computational complexity have been widely used for the acquisition of binary phase shift keying (BPSK) global positioning system (GPS) signals. In this paper, we propose a low computational FFT-based fine acquisition technique, for binary offset carrier (BOC) modulated BPSK signals, that depending on the subcarrier-to-code chip rate ratio (SCR) selectively utilizes the computationally efficient frequency-domain realization of the BPSK-like technique and two-dimensional compressed correlator (BOC-TDCC) technique in the first stage in order to achieve a fast coarse acquisition and accomplishes a fine acquisition in the second stage. It is analyzed and demonstrated that the proposed technique requires much smaller mean fine acquisition computation (MFAC) than the conventional FFT-based BOC acquisition techniques. The proposed technique is one of the first techniques that achieves a fast FFT-based fine acquisition of BOC signals with a slight loss of detection probability. Therefore, the proposed technique is beneficial for the receivers to make a quick position fix when there are plenty of strong (i.e., line-of-sight) GNSS satellites to be searched.

Keywords: BOC, FFT-based, two-dimensional compressed correlator

1. INTRODUCTION

The coarse/acquisition (C/A) code signal of the global positioning systems (GPS) uses a binary phase shift keying (BPSK) modulated pseudo-random noise (PRN) code of 1023 chips long. Since GPS satellites are orbiting the earth with a velocity about 3.92 km/s, and the center frequency of the C/A code signal is L_1=1.57542 GHz, the Doppler frequency of a GPS signal arriving at the earth surface can be anywhere within [-5, 5] kHz (Kaplan & Hegarty 2006). For continuous positioning, the acquisition function in a GPS receiver needs to find the true code phases and Doppler frequencies of all incoming GPS signals and the tracking function is successfully tracking the acquired GPS signals. Since the code phase and Doppler frequency search step sizes in the acquisition function are 0.5 chips and 500 Hz in many receivers, respectively, the GPS acquisition function needs to test a huge number of code phase and Doppler frequency hypotheses in a two-dimensional (2D) hypothesis space, which is, therefore, a computationally expensive and time consuming process.

Among a number of GPS acquisition techniques developed and introduced in the literature (Borre et al. 2007, Kong & Kim 2013), parallel acquisition techniques based on multiple parallel correlators (matched filters) have been widely used to speed up the acquisition at the cost of increased hardware complexity in the receiver (Borre et al. 2007). And the fast Fourier transform (FFT)-based technique implemented in a digital signal processor (DSP) (Akopian 2005, Borre et al. 2007) has become one of the most popular parallel acquisition techniques. To

Received Feb 25, 2022 **Revised** Mar 03, 2022 **Accepted** Mar 07, 2022
[†]**Corresponding Author**
E-mail: skong@kaist.ac.kr
Tel: +82-42-350-1265 Fax: +82-42-350-1250
Jeong-Hoon Kim https://orcid.org/0000-0001-9996-9396
Binhee Kim https://orcid.org/0000-0002-9077-7061
Seung-Hyun Kong https://orcid.org/0000-0002-4753-1998

 http://www.ipnt.or.kr Print ISSN: 2288-8187 Online ISSN: 2289-0866

reduce the hardware complexity and the mean acquisition computation (MAC) of the FFT-based techniques, a number of signal processing algorithms have been introduced in the literature. For example, average correlator (AC) (Yi et al. 2008) can reduce FFT size by averaging over-sampled received signal, and the shifting replica (SR) (Akopian 2005) can reduce the frequency-domain complex multiplications when multiple period of the PRN code is correlated. In folding and dual-folding techniques (Yang et al. 1999, Li et al. 2008), locally generated PRN code sequence and incoming global navigation satellite systems (GNSS) signal are folded, respectively, and correlated in the frequency-domain to reduce the computational cost and time at the cost of Signal-to-Noise Ratio (SNR) degradation proportional to the number of folding. In Kong & Kim (2013) and Kim & Kong (2014b), two-dimensional compressed correlator (TDCC) and FFT-based TDCC are introduced for the serial and the frequency-domain parallel search of BPSK signals to reduce the mean acquisition time (MAT) and the mean acquisition computation (MAC), respectively.

In GNSS, there are various BOC signals that is BPSK signals modulated by binary offset carrier BOC(m_{sc}, m_c) (Julien et al. 2007, Dovis et al. 2008, Borio 2011), for example, BOC(1, 1), BOC(10, 5), BOC(15, 2.5), and BOC(14, 2). Accordingly, studies for fast BOC signal acquisition have been introduced in the literature recently; deterministic compressed acquisition (DCA) technique (Kong 2013) for BOC(1, 1) signals, and the time-domain TDCC technique for various BOC(m_{sc}, m_c) signals (BOC-TDCC in short) (Kim & Kong 2014a). However, up to the present, there has been little study to develop computationally efficient FFT-based fine acquisition technique for BOC signals. In addition, to reduce algorithmic complexity to handle multiple sign changes within a chip appearing in the auto-correlation function (ACF) output of BOC signals, BOC acquisition techniques such as single-sideband (SSB) and double-sideband (DSB) aim to achieve only the coarse acquisition of BOC signals, i.e., detecting the code phase with a half code chip resolution (Fishman & Betz 2000). The BPSK-like technique utilizing the SSB of the BOC signal spectrum achieves a coarse acquisition and an additional fine acquisition, i.e., detecting the code phase with a half subcarrier chip resolution, is required for the immediate start of the BOC tracking function.

In this paper, we show that the modified FFT-based BOC-TDCC, the FFT-based fine acquisition of BOC signals utilizing the BOC-TDCC (Kim & Kong 2014a) modified with spectrum segmentation and folding (SSF), and the FFT-based BPSK-like technique achieves a low computational acquisition of BOC signals depending on the subcarrier-to-code chip rate ratio (SCR) of the BOC signal. Exploiting that the FFT-based BPSK-like technique has more computational advantage over the modified FFT-based BOC-TDCC for higher SCR, we propose a low computational FFT-based fine BOC signal acquisition technique that selectively utilizes the BPSK-like (Margaria et al. 2008) technique and the modified FFT-based BOC-TDCC technique depending on the SCR in the first stage to achieve a fast coarse acquisition. The proper selection to the technique to be used in the first stage depends on the SCR and is theoretically analyzed. In the second stage, the proposed technique exploits the conventional correlators to finalize the fine acquisition of the BOC signal. The proposed technique is one of the first FFT-based fast fine acquisition techniques for BOC signals, and it is demonstrated that the proposed technique achieves multiple times smaller computational cost in the acquisition of BOC signals than conventional FFT-based technique.

There is an additional benefit with the proposed technique. At present, the number of visible GNSS satellites is increasing as new satellites are launched to their orbits and is expected to be higher than 60 at any location on earth surface. In this case, a GNSS receiver may need to quickly search line-of-sight (LOS) satellites rather than try to detect weak GNSS satellites, since there are plenty of LOS satellites in the sky. Therefore, a GNSS acquisition technique that enables fast (i.e., low computational) acquisition of strong LOS satellites is strongly required by the commercial market. The proposed technique demonstrates maximum 10 times lower computational cost with slight lower detection probability than the conventional acquisition techniques for LOS GNSS signals.

The rest of this paper is organized as follows. Section 2 introduces an overview of the proposed low computational FFT-based fine BOC signal acquisition technique depending on the SCR. Section 3 and Section 4 show the BPSK-like-based (i.e., proposed-1 technique) and the modified TDCC-based (i.e., proposed-2 technique), respectively, used for the fast coarse acquisition. Section 5 shows the computational complexity and performance analysis of the proposed technique. Theoretical analysis of the SCR-based selection is derived in Section 6, and the performance of the proposed technique is demonstrated with numerous Monte Carlo simulations and comparisons to the conventional FFT-based BOC(m_{sc}, m_c) acquisition technique are provided and discussed in Section 7. Finally, our conclusion is drawn in Section 8.

The following notations are used throughout this paper. Vectors or matrices are denoted by boldface symbols. Frequency domain signals are denoted by capital letters,

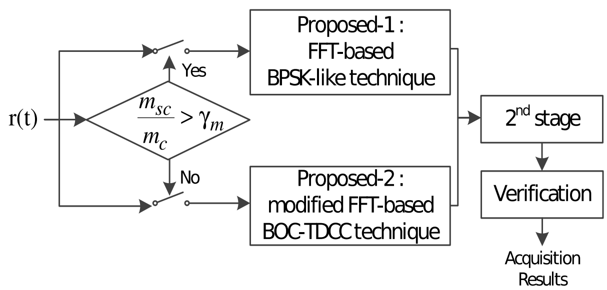

Fig. 1. Schematic diagram of the proposed technique.

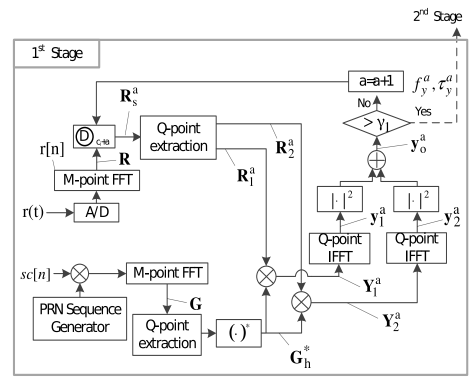

Fig 2. Proposed-1: FFT-based BPSK-like technique.

and time domain signals are denoted by small letter.

2. OVERVIEW OF LOW COMPUTATIONAL BOC ACQUISITION

Let $r(t)$ be a BOC(m_{sc}, m_c) signal arriving at a ground GNSS receiver as

$$r(t) = AD(t-\tau)P_m(t-\tau)sc_m(t-\tau)e^{j(2\pi(f_{IF}+f_D)t+\theta)} + w(t) \quad (1)$$

where A, $D(t)$ and $P_m(t)$ represent the amplitude, data at R_b bps, and PRN code at a code rate $R_c(=m_c f_r=1/T_c)$ [Hz], respectively, $m_c>0, f_r$=1.023 MHZ is the reference frequency, $sc_m(t)$ represents the subcarrier function with a subcarrier frequency $f_{sc}(=m_{sc}f_r)$ [Hz] for $m_{sc}\geq m_c$ as

$$sc_m(t) = \begin{cases} \text{sgn}(\sin(2\pi f_{sc}t)), for \sin BOC \\ \text{sgn}(\cos(2\pi f_{sc}t)), for \cos BOC, \end{cases} \quad (2)$$

and τ, f_{IF}, f_D, θ and $w(t)$ represent the code phase, intermediate frequency (IF), Doppler frequency, unknown carrier phase of the incoming signal and a complex AWGN noise with two-sided power spectral density $\frac{N_0}{2}$, respectively. The ratio $2m_{sc}/m_c$ is constrained to be a positive integer (Julien et al. 2007).

BPSK-like technique (Fishman & Betz 2000) uses a bandpass filter (BPF) to process one of the two main lobes of the BOC spectrum in the acquisition, where the sampling frequency and the computational cost can be reduced at the cost of SNR loss. The advantage of the BPSK-like technique increases as the SCR, i.e., m_{sc}/m_c, increases. On the other hand, when the SCR is small, the advantage of the modified FFT-based BOC-TDCC that we propose in Section 3 is stronger than the BPSK-like technique.

Fig. 1 shows the overall diagram of the proposed technique that utilizes the FFT-based BPSK-like technique and the modified FFT-based BOC-TDCC technique depending on the SCR; When the decision threshold γ_m is smaller than the SCR, the proposed technique switches to the BPSK-like technique. The performance of the proposed technique with respect to the decision threshold is theoretically analyzed and tested in Section 6, where the proper value of γ_m is defined. In the following, proposed-1 technique and proposed-2 technique denote the FFT-based BPSK-like technique and the modified FFT-based BOC-TDCC technique, respectively. Note that in Fig. 1 the proposed-1 and proposed-2 techniques are for the first stage, where a coarse acquisition of the BOC signal is performed, i.e., code chip level acquisition, and that the second stage employs the conventional correlation-based search for a fine acquisition, i.e., subcarrier chip level acquisition.

3. PROPOSED-1: FFT-BASED BPSK-LIKE TECHNIQUE

In this section, we propose a FFT-based BPSK-like technique (proposed-1 technique). The overall process of the proposed-1 technique can be easily explained with a schematic diagram in Fig. 2, where the operation $\textcircled{D}_k$ represents the circular shift of k samples. The incoming signal $r[n]$ is first FFT'd as

$$R[k] = \sum_{n=0}^{M-1} r[n]e^{-j2\pi kn/M}, \quad (3)$$

where k=0, 1, ⋯, M-1, M is the number of FFT-points and is the smallest power of 2 integer larger than $2vN$ (Yang 2001), $v=f_s/R_c$, N is the number of code chips in one PRN period. And $R[k]$ is circular shifted to search for Doppler frequency hypotheses as

$$R_S^a[k] = R[k+c_i+a], \quad (4)$$

where c_i denotes the index of the smallest individual Doppler frequency hypothesis, and a denotes the additionally increased index for the Doppler frequency hypotheses. To deal with BPSK-like signal, two main lobes of the BOC signal are captured as

$$\mathbf{R}_1^a = \mathbf{R}_s^a[Qm_F/2+1:Q(m_F/2+1)] \tag{5a}$$

$$\mathbf{R}_2^a = \mathbf{R}_s^a[Q(3m_F/2+1)+1:Q(3m_F/2+2)], \tag{5b}$$

where Q is the number of FFT-points and is the smallest positive integer that is a power of 2 larger than $2N$ (Yang 2001), $m_F=2^{\log_2 M-\log_2 Q-1}-1$. Same as the process of an incoming signal, FFT-transformed locally generated signal G is also captured to generate BPSK-like signal as

$$\mathbf{G}_h = \mathbf{G}[Q(3m_F/2+1)+1:Q(3m_F/2+2)]. \tag{6}$$

To correlate the incoming signal and locally generated signal, R_1^a $[k]$ and R_2^a $[k]$ are multiplied with the complex conjugate of G_h $[k]$ to produce Y^a $[k]$ as

$$Y_1^a[k] = R_1^a[k]G_h^*[k], \tag{7a}$$

$$Y_2^a[k] = R_2^a[k]G_h^*[k], \tag{7b}$$

and Y_1^a and Y_2^a are IFFT transformed to get

$$y_1^a[n] = \sum_{k=0}^{Q-1} Y_1^a[k]e^{j2\pi kn/Q}, \tag{8a}$$

$$y_2^a[n] = \sum_{k=0}^{Q-1} Y_2^a[k]e^{j2\pi kn/Q}, \tag{8b}$$

and squares of Y_1^a and Y_2^a are summed as

$$y_o^a[n] = |y_1^a[n]|^2 + |y_2^a[n]|^2. \tag{9}$$

Denoting a_0 as the frequency hypotheses index of y_0^a whose element is larger than the decision threshold, γ_1, the index of the detected code phase hypothesis τ_y^a and the index of the detected Doppler frequency hypothesis f_y^a can be expressed as

$$\tau_y^a = \arg\max_n |\mathbf{y}_o^{a_0}| \tag{10a}$$

$$f_y^a = a_0 \tag{10b}$$

where $\tau_y^a \in \left\{0,\cdots,\left\lceil\frac{4m_{sc}QN}{m_cM}\right\rceil-1\right\}$ and $f_y^a \in \{0,\cdots,F_n-1\}$, F_n is the number of individual Doppler frequency hypotheses, and the corresponding individual code phase to be tested in the second stage exploiting conventional correlators is $\tau_y^a(2m_{sc}/m_c)+m_s^a$, where $m_s^a\in\{0,\cdots,2\,m_{sc}/m_c-1\}$ is the index of the corresponding individual code phase hypotheses that constitute the detected hypothesis in the first stage.

4. PROPOSED-2: MODIFIED FFT-BASED BOC-TDCC TECHNIQUE

In this subsection, we develop the modified FFT-based BOC-TDCC technique (proposed-2 technique) (Kim & Kong 2014a) and derive mathematical expressions. The overall process of the proposed-2 technique is shown in Fig. 3.

For BOC signals, a compressed code phase signal with c_c neighboring code phase hypotheses with a half chip spacing is generated as

$$g_f[n] = \sum_{d=0}^{c_c-1} (-1)^d g[n-v_n d], \tag{11}$$

where $(-1)^d$ is to compensate the alternating signs in the ACF output, $v_n=v_{mc}/(2\,m_{sc})$ is the number of samples per a sub-chip (i.e., a half period of a subcarrier), $g[n]$ is a locally generated PRN code as shown in Fig. 3b. And then, as shown in Fig. 3a, FFT of the compressed code phase signal $g_f[n]$ yields

$$G_f[k] = \sum_{n=0}^{M-1} g_f[n]e^{-j2\pi kn/M}. \tag{12}$$

As shown in Fig. 3c, for compression of neighboring Doppler frequency hypotheses with $\frac{1}{2\mathrm{T}}$ Hz spacing, the incoming signal $r[n]$ is M-point FFT'd to yield $R[k]$, and c_f consecutive $R[k]$s are coherently combined with $\pi/2$ phase compensation between neighboring Doppler frequency hypotheses and, then, circular shifted to test the next coherently combined c_f Doppler frequencies at $c_f\Delta f$ apart (Akopian 2005) as

$$R_s^b[k,h] = \sum_{a=0}^{c_f-1} R\big[k+c_i+c_fh+b\big]e^{-j\pi b/2}, \tag{13}$$

where $h \in \{0,\cdots,\lceil F_n/c_f\rceil-1\}$, and b denotes the additionally increased index of the Doppler frequency hypothesis. As in Fig. 3a, to correlate the incoming signal with the receiver replica signal, $R_s^b[k,h]$ and the complex conjugate of $G_f[k]$ is multiplied to produce $Y^b[k,h]$ as

https://doi.org/10.11003/JPNT.2022.11.1.11

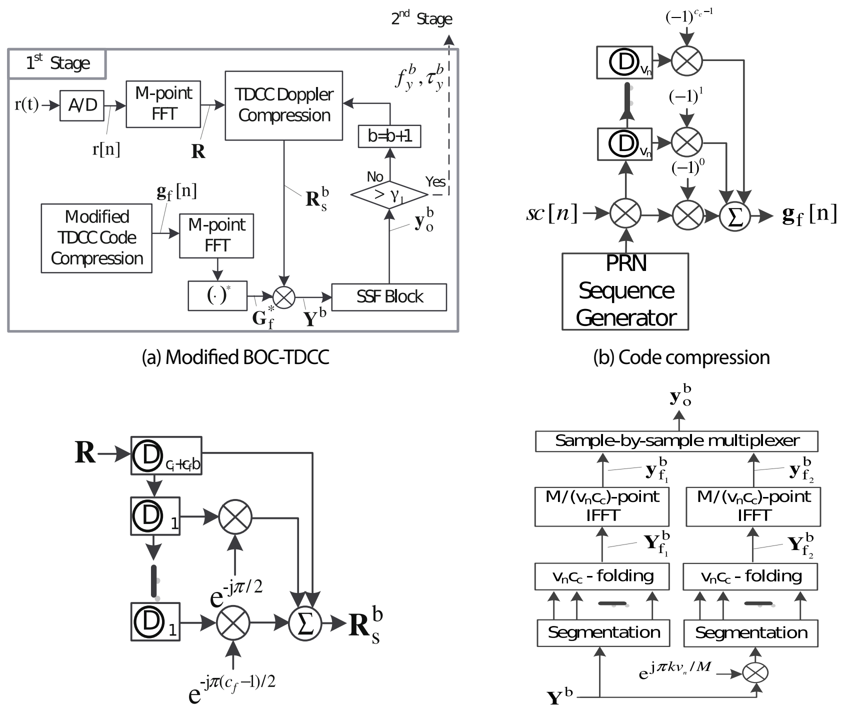

(a) Modified BOC-TDCC (b) Code compression

(c) Doppler compression (d) Spectrum segmentation and folding (SSF)

Fig. 3. Proposed-2: Modified FFT-based BOC-TDCC technique.

$$Y^b[k,h] = R^b_s[k,h] G^*_f[k]. \tag{14}$$

Since a compressed PRN code sequence is composed of c_c PRN code sequences whose code phases are $1/(2f_{sc})$, the ACF output samples, i.e., the time-domain element of Y^b, should be down-sampled. The equivalent down-sampling operation in the time-domain is realized by taking every $(v_n c_c i+1)$-th samples and $(v_n c_c i+2)$-th samples of the ACF output for i=0, 1, ⋯, $\lfloor (vN)/(v_n c_c) \rfloor$. The down-sampling process is to reduce the number of IFFT points for computational saving, since IFFT should be performed for every compressed Doppler frequency hypotheses. Using $f_s=4f_{sc}$ and assuming mod(M,c_c)=0 for an algebraic simplicity, the first samples of every $v_n c_c$ samples of $y^b[n,h]$ are

$$y^b_{f_1}[n,h] = y^b[v_n c_c n, h] = \sum_{k=0}^{M-1} Y^b[k,h] e^{j2\pi(v_n c_c n)k/M} = \sum_{k=0}^{M/(v_n c_c)-1} \left(\sum_{q=0}^{v_n c_c -1} Y^b\left[k + \frac{M}{v_n c_c} q, h\right] \right) e^{j2\pi(v_n c_c)nk/M}, \tag{15}$$

and the second samples of every $v_n c_c$ samples of $y^b[n,h]$ are

$$y^b_{f_2}[n,h] = y^b[v_n c_c n + v_n/2, h] = \sum_{k=0}^{M-1} Y^b[k,h] e^{j2\pi(v_n c_c n + v_n/2)k/M} = \sum_{k=0}^{M-1} \left(Y^b[k,h] e^{j\pi v_n k/M}\right) e^{j2\pi(v_n c_c n)k/M} = \sum_{k=0}^{M/(v_n c_c)-1} \left(\sum_{q=0}^{v_n c_c -1} Y^b\left[k + \frac{M}{v_n c_c} q, h\right] e^{j\pi v_n \left[k + \frac{M}{v_n c_c} q\right]/M} \right) e^{j2\pi(v_n c_c)nk/M}, \tag{16}$$

where f_1 and f_2 represent the first and second sample sets, respectively, as shown in Fig. 3d. Note that $y^b_{f_1}[n,h]$ and $y^b_{f_2}[n,h]$ represent the test results of two hypotheses within a sub-chip. To complete the down-sampling process in Eqs. (15) and (16), Y^a should be divided into v_n segments, and each segment is $v_n c_c$ times folded before the IFFT operation. The folded first sample set in the frequency-domain

$$Y^b_{f_1}[k,h] = \sum_{l=0}^{v_n c_c -1} Y^b\left[k + \frac{Ml}{v_n c_c}, h\right], \tag{17}$$

and the folded second sample set in the frequency-domain

$$Y_{f_2}^b[k,h] = \sum_{l=0}^{v_n c_c - 1} Y^b\left[k + \frac{Ml}{v_n c_c}, h\right] e^{j2\pi v_n\left(k+\frac{Ml}{v_n c_c}\right)/(2M)} \quad (18)$$

are inverse FFT'd to obtain the first stage result as

$$y_{f_i}^b[n,h] = \sum_{k=0}^{M/(v_n c_c)-1} Y_{f_i}^b[k,h] e^{j2\pi kn/(M/(v_n c_c))}. \quad (19)$$

As in Fig. 3d, the components of y^b_{f1} and y^b_{f2} are arranged in order to find y^b_o as

$$y_o^b[n,h] = \left(\mathrm{mod}(n,2) y_{f_1}^b\left[\left\lfloor\frac{n}{2}\right\rfloor, h\right]\right) + \left(\mathrm{mod}(n+1,2) y_{f_2}^b\left[\left\lfloor\frac{n}{2}\right\rfloor, h\right]\right), \quad (20)$$

and each component of y^b is compared to the first stage detection threshold γ_1 as shown in Fig. 3a.

When a test result for a compressed hypothesis is larger than γ_1, the index of the detected compressed Doppler frequency hypothesis f_y^b and the index of the detected compressed code phase hypothesis τ_y^b are sent to the second stage, where the corresponding $c_c c_f$ neighboring individual hypotheses are tested. Denoting b_0 as the compressed frequency hypotheses index of y_o^b whose element passes the decision threshold test, the index of the detected compressed code phase hypothesis τ_y^b and the index of the detected compressed Doppler frequency hypothesis f_y^b can be expressed as

$$\tau_y^b = \arg\max_n \left|\mathbf{y}_o^{b_0}\right| \quad (21a)$$

$$f_y^b = b_0, \quad (21b)$$

where $\tau_y^b \in \left\{0, \cdots, \left[\frac{4Nm_{sc}}{c_c m_c}\right] - 1\right\}$ and $f_y^b \in \left\{0, \cdots, \left[\frac{F_n}{c_f}\right] - 1\right\}$, and the indices of the resulting individual code phase and Doppler frequency hypotheses to be tested in the second stage are $v_n c_c \left\lfloor\frac{\tau_y^b}{c_c}\right\rfloor + \mathrm{mod}(\tau_y^b, 2)\frac{v_n}{2} + v_n m_s^b - 1$ and $c_i + f_y c_f + n_s^b$, respectively, where $m_s^b \in \{0, \cdots, c_c - 1\}$ and $n_s^b \in \{0, \cdots, c_f - 1\}$ are the indices of the individual code phase and Doppler frequency hypotheses that constitutes the detected compressed hypothesis in the first stage.

5. PERFORMANCE ANALYSIS

In this section, the computational complexity and performance analysis of the proposed technique are explained.

5.1 Computational Complexity

Since the indices of Doppler frequency hypotheses are denoted a in the proposed-1 technique, we express the code search with the Doppler frequency hypothesis by a-th code search. Therefore the number of complex multiplications of the a-th code search in the first stage of the proposed-1 technique is

$$N_f^a = 2Q(1 + \log_2 Q). \quad (22)$$

On the other hand, similar to the proposed-1 technique, the number of complex multiplications of b-th code search in the proposed-2 technique is

$$N_f^b = (c_f - 1)M + 2M + \frac{M}{c_c}\log_2\frac{M}{2c_c}. \quad (23)$$

And it is known that the number of complex multiplications of the code search in the conventional FFT-based BOC acquisition technique (Borre et al. 2007) is

$$N_v = M + M\log_2 M. \quad (24)$$

The computation in the second stage for the proposed-1 and proposed-2 technique can be expressed as

$$N_s^a = vN(1 + m_{sc}/m_c), \quad (25a)$$

$$N_s^b = vN\left(min\{c_c, c_f\} + c_c c_f\right), \quad (25b)$$

respectively. The total computational complexity of the proposed and the conventional FFT-based BOC acquisition technique (Borre et al. 2007) are analyzed and simulated in Section 6 and Section 7, respectively.

5.2 Mean Fine Acquisition Computation

In order to verify the performance of the proposed technique, thorough theoretical analysis is introduced in this section. Since the performance of the BPSK-like technique is already introduced in Fishman & Betz (2000), we provide the performance analysis of the modified FFT-based BOC-TDCC (proposed-2) technique in this section.

From Kim & Kong (2014a), the noise power, σ_P^2, due to the compressed code phase hypothesis, is a function of m_{sc}/m_c and c_c as

$$\sigma_P^2 = \begin{cases} 4 - m_c/m_{sc}, & \text{for } c_c = 2 \text{ and } m_{sc}/m_c > 1 \\ 16 - 10\, m_c/m_{sc}, & \text{for } c_c = 4 \text{ and } m_{sc}/m_c > 1 \\ 64 - 84\, m_c/m_{sc}, & \text{for } c_c = 8 \text{ and } m_{sc}/m_c > 3, \end{cases} \quad (26)$$

and 3, 7, 14, 27, 109/3 for $[c_c, m_{sc}/m_c]$= [2,1], [4,1], [8,1], [8,2], and [8,3], respectively, and the noise power due to the compressed Doppler frequency hypothesis denoted by σ_f^2 is $2+\frac{4}{\pi}$ for c_f=2, $3+\frac{8}{\pi}$ for c_f=3, and $4+\frac{32}{3\pi}$ for c_f=4 (Kong 2013), where the noise of the first stage IFFT output is $V_1=\sigma_f^2\sigma_p^2 \upsilon NN_0$, and that of the second stage output is $V_2=\upsilon NN_0$. And the signal amplitude of $y_o^{b}[\tau_y^b]$ is denoted as S_1 defined in Kim & Kong (2014a).

To test if the first stage acquisition is successful, we use the maximum-to-the second maximum ratio (MTMR)-based decision strategy introduced in Geiger et al. (2010), where the ratio of MTMR of the parallel search output is compared to a decision threshold γ_1. Then, the detection probability, miss probability, false alarm probability in the incorrect Doppler frequency hypothesis, and false alarm probability in the correct Doppler frequency hypothesis are

$$P_D^1 = e^{-\frac{s_1^2}{2}} \sum_{q=0}^{\infty} \left[\frac{(S_1^2)^q}{2_q q!} \right. \\ \left. {}_{q+2}F_{q+1}\left([-N_r, \gamma_1 \mathbf{1}_{q+1}]; (\gamma_1+1)\mathbf{1}_{q+1}; 1\right) \right] \tag{27a}$$

$$P_M^1 = 1 - P_D^1 - P_f^1 \tag{27b}$$

$$P_F^1 = (N_1^2 - N_1) B(N_1 - 1, 1 + \gamma_1), \tag{27c}$$

and

$$P_f^1 = \begin{cases} 0, & for\ high\ SNR \\ (N_1^2 - N_1)B(N_1 - 1, 1 + \gamma_1), & for\ low\ SNR, \end{cases} \tag{28}$$

respectively, where $B(\cdot,\cdot)$ is the Beta function (Papoulis & Pillai 2002), ${}_pF_q([a_1,\cdots,a_p];[b_1,\cdots,b_q];1)$ is hypergeometric series, and 1_n is an 1-by-n matrix of ones. In the second stage, the detection, miss, and false alarm probabilities are readily available from the literature such as (Kong 2013)

$$P_D^2 = \sum_{n=0}^{N_2-1} \frac{(-1)^n}{n+1} \binom{N_2-1}{n} \exp\left(-\frac{nS_2^2}{(n+1)V_2}\right) \\ Q\left(\sqrt{\frac{2S_2^2}{(n+1)V_2}}, \sqrt{\frac{2(n+1)\gamma_2}{V_2}}\right), \tag{29a}$$

$$P_M^2 = \left(1 - \exp\left(-\frac{\gamma_2}{V_2}\right)\right)^{N_2-1} \left[1 - Q\left(\sqrt{\frac{2S_2^2}{V_2}}, \sqrt{\frac{2\gamma_2}{V_2}}\right)\right], \tag{29b}$$

$$P_F^2 = 1 - \left(1 - \exp\left(-\frac{\gamma_2}{V_2}\right)\right)^{N_2}, \tag{29c}$$

where $N_2=c_c c_f$.

The correct hypothesis detection, the correct hypothesis missed, and the incorrect hypothesis branch transfer functions related to the computational complexity in the acquisition process can be derived as (Viterbi 1995, Kim & Kong 2014b)

$$H_D^c(C) = P_D^1 P_D^2 P_D^V C^{N_f} C^{N_s} C^{N_p} \tag{30a}$$

$$H_M^c(C) = P_M^1 C^{N_f} + (1 - P_D^1 - P_M^1)(1 - P_F^2) C^{N_f} C^{N_s} \\ + \left((1 - P_D^1 - P_M^1) P_F^2 + P_D^1 P_f^2\right) \\ \times \left(1 - P_f^v\right) C^{N_f} C^{N_s} C^{N_p} \tag{30b}$$

$$H_0^c(C) = (1 - P_F^1 P_F^2) C^{N_f} C^{N_s} \\ + (P_F^1 P_F^2)(1 - P_F^v) C^{N_f} C^{N_s} C^{N_p}, \tag{30c}$$

respectively, where N_p is the penalty computations required for the verification process. Exploiting the analysis in Viterbi (1995), the overall transfer function related to the computational complexity in the proposed technique is

$$H^c(C) = \frac{H_D^c(C)\left[1 - H_0^{cF_c}(C)\right]}{F_c\left[1 - H_0^c(C)\right]\left[1 - H_M^c(C) H_0^{c(F_c-1)}(C)\right]}, \tag{31}$$

and the mean fine acquisition computation (MFAC) can be derived as

$$\mu_C = \frac{P_D^1 P_D^2 C}{P_D^1 - P_D^1 P_f^2} \\ \left(N_f + N_s + N_p + \frac{F_c - 1}{2}\left(N_p P_F^1 P_F^2 + N_f + N_s P_F^1\right)\right) \\ + \frac{P_D^2 C}{P_D^1\left(1 - P_f^2\right)^2}\left(N_f P_M^1 + \left(N_f + N_s + N_p\right) P_D^1 P_f^2 \right. \\ + \left(N_f + N_s + pP_F^2\right)\left(1 - P_D^1 - P_M^1\right) \\ \left. + (F_c - 1)\left(1 - P_D^1 + P_D^1 P_f^2\right)\left(N_p P_F^1 P_F^2 + N_f + N_s P_F^1\right)\right), \tag{32}$$

where fine acquisition means that resolution for the acquisition is subcarrier sub-chip. Note that, for a high SNR, the expression Eq. (32) simplifies to

$$\mu_C \simeq \frac{F_c + 1}{2} N_f + N_s + N_p \tag{33}$$

6. THEORETICAL ANALYSIS OF THE SCR-BASED SELECTION

The mean acquisition computation of the proposed-1 and proposed-2 techniques in Section 4 vary with respect to m_{sc}/m_c of the BOC signal. A proper choice of the decision threshold γ_m is to achieve the minimum MAC for high SNR, when the goal of the acquisition is to acquire as many strong LOS satellites as quickly as possible to determine a position

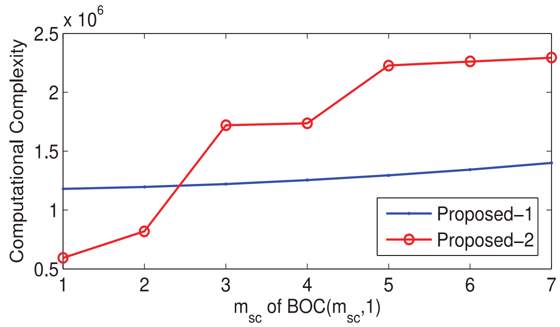

Fig 4. Computational complexity for high SNR.

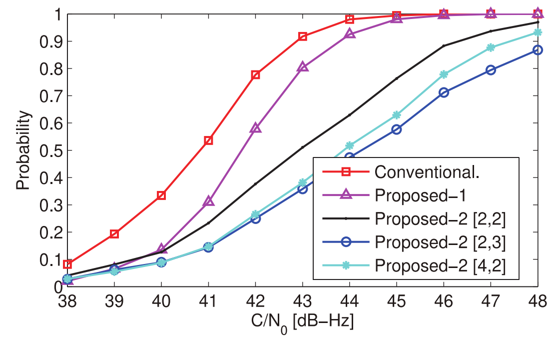

Fig 5. Detection probability of BOC(2, 1).

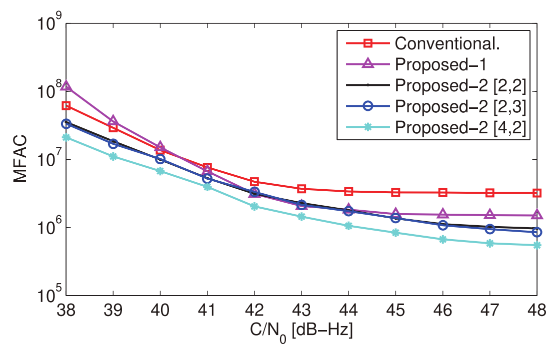

Fig 6. Mean fine acquisition computation of BOC(2, 1).

fix. To determine γ_m, we use Eqs. (22), (23), (25a), (25b), and (33) to find some simulation results shown in Fig. 4, where c_c and c_f of the proposed-2 technique is determined such that the maximum SNR loss is less than 2 dB. For example, $[c_c, c_f]$ = [2, 1] for BOC(1, 1), $[c_c, c_f]$=[2, 2] for BOC(2, 1), BOC(3, 1), and BOC(4, 1), and $[c_c, c_f]$= [4, 2] for BOC(5, 1), BOC(6, 1) and BOC(7, 1). As shown, the proposed-2 technique has smaller MAC for SCR less than 3, whereas the proposed-1 technique has smaller MAC for SCR larger than 2. Therefore, it can be found that γ_m=2.5 without loss of generality. In practice, proposed-1 technique shall be useful for the low computational acquisition of GPS L1-M, Galileo E6-A, GPS L2-M, Galileo E1 BOC(1, 1), COMPASS B1 BOC(1, 1), and proposed-2 technique shall be useful for the low computational acquisition of COMPASS B1, Galileo E1-A, COMPASS B3-A_D, and COMPASS B3-A_P.

7. NUMERICAL RESULTS

In this section, the proposed acquisition technique tested for a receiver, with $4f_{sc}$ Hz BPF bandwidth, sampling frequency f_s=$4f_{sc}$ and correlation interval T=1 msec. The code phase and Doppler frequency search step sizes are $(T_c m_c)/(4m_{sc})$ and Δf=500 Hz, respectively, and the chip rate of the PRN code is Rc=1.023 MHz, the chip rate of the tiered code is 1 kHz, and Doppler frequency search is from -5 kHz to 5 kHz. In the following simulations, we target the constant false alarm rate, P_F=10^{-2} (Spangenberg et al. 2000, Li et al. 2008), and the decision threshold γ_i for the i-th stage is set from P_F^i in Eqs. (27c) and (29c) as Ye et al. (2008).

Fig. 5 shows a result of 104 Monte Carlo simulations for the detection probabilities of sinBOC(2, 1) for the proposed acquisition techniques. As shown in Eq. (27a), the detection probability decreases as $c_c c_f$ increases. The detection probability for the proposed-1 technique is about 1 dB less than that for the conventional FFT-based BOC acquisition technique, and the detection probability for the proposed-2 technique with $[c_c, c_f]$ = [2, 2] is 3 dB less than that for the conventional FFT-based BOC acquisition technique.

Fig. 6 shows the MFAC of the proposed acquisition techniques for sinBOC(2, 1) evaluated from 10^4 Monte Carlo simulations, where the MFAC is the average number of total complex multiplications performed until a fine signal acquisition is declared at the verification process which performs p (=10) times computations. The proposed acquisition technique compared with the conventional FFT-based BOC acquisition technique (Borre et al. 2007). As expected, the MFAC for the fine acquisition decreases as C/N_0 increases, and the code phase hypothesis compression c_c has a great impact on the computational complexity. For high C/N_0, the proposed-2 technique with $[c_c, c_f]$ = [2, 2] requires less than 70% and 30% of the MFAC required for the conventional FFT-based BOC acquisition technique and proposed-1 technique, respectively. As C/N_0 decreases, the MFAC of all the acquisition technique starts to increase. Especially, the MFAC of the proposed-2 technique becomes higher than that of the conventional FFT-based BOC acquisition technique (Borre et al. 2007) at C/N_0=40 dB-Hz. For moderate C/N_0 (e.g., <42 dB), the proposed-2 technique with $[c_c, c_f]$ = [4, 2] requires about 30% of MFAC used by the conventional FFT-based BOC acquisition technique (Borre et al. 2007).

Fig. 7 shows a result of 10^4 Monte Carlo simulations for

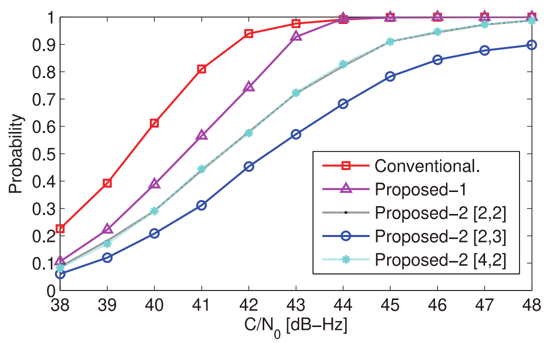

Fig 7. Detection probability of BOC(7,1).

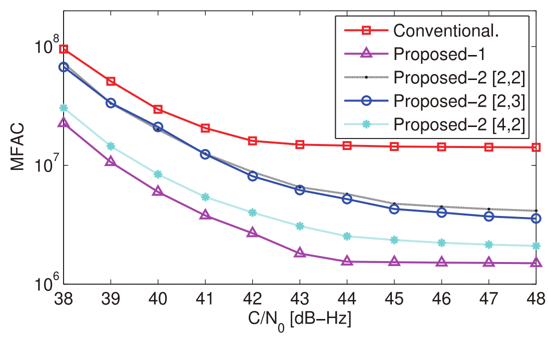

Fig 8. Mean fine acquisition computation of BOC(7, 1).

the detection probabilities of sinBOC(7, 1) for various c_c and c_f in the first stage of the proposed-2 technique. As shown in Eq. (27a), the detection probability decreases as $c_c c_f$ increases. The detection probability for the proposed-1 technique is about 1 dB less than that for the conventional FFT-based BOC acquisition technique, which is similar to the case of sinBOC(2, 1). However, the difference of detection probability between the proposed-2 technique with $[c_c, c_f]$ = [2, 2] and the conventional FFT-based BOC acquisition technique is much smaller than that for sinBOC(2, 1). This is because non-negligible energy at the neighboring code phases of the true code phase increases as SCR increases.

Fig. 8 shows the MFAC of the proposed acquisition techniques for sinBOC(7, 1) evaluated from 10^4 Monte Carlo simulations, where the simulation environment is same as that for Fig. 6. As expected, the MFAC for the signal acquisition decreases as C/N_0 increases, and the code phase hypothesis compression c_c has a great influence on the computational complexity for the proposed-2 technique. The performance of the proposed-1 technique for sinBOC(7, 1) is much better than that for sinBOC(2, 1). For high C/N_0, the proposed-1 technique requires less than 75% and 40% of the proposed-2 technique with $[c_c, c_f]$ = [4, 2] and $[c_c, c_f]$ = [2, 3], respectively. As C/N_0 decreases, the MFAC of all the acquisition techniques starts to increase. For moderate C/N_0 (<42 dB), the proposed-1 technique and the proposed-2 technique with $[c_c, c_f]$ = [4, 2] requires about 20% and 30% of MFAC used by the conventional FFT-based BOC acquisition technique, respectively (Borre et al. 2007). The MFAC of the proposed-1 technique outperforms that of the proposed-2 technique for sinBOC(7, 1) due to high SCR.

Note that, as shown in Figs. 5 and 7, the degradation of the detection probability for LOS satellites (i.e., C/N_0 > 44 dBHz) in comparison to the conventional technique is negligible for the proposed-1 technique but non-negligible for the proposed-2 technique. However, as shown in Figs. 6 and 8, the computational cost in comparison to the conventional technique is significant for the proposed-1 technique; the reduction of computational cost is about 2 times in Fig. 6 and about 10 times in Fig. 8. This result demonstrates that the proposed technique (especially, the proposed-1 technique) enables a fast and efficient acquisition of LOS satellites, which can reduce the requirement for computational capacity of the GNSS receivers.

8. CONCLUSION

A low computational FFT-based fine BOC signal acquisition technique depending on SCR has been presented in this paper. The first stage of the proposed technique selectively utilizes the frequency-domain realization of BPSK-like and modified BOC-TDCC techniques depending on the SCR in order to achieve a low computational and fast coarse acquisition of the incoming BOC signal, and the second stage completes the fine BOC acquisition. The proper choice of acquisition technique for the first stage has been determined from the theoretical analysis of the MAC. The performance of the proposed technique has been theoretically analyzed and demonstrated with numerous Monte Carlo simulations. It has been shown that the proposed techniques achieve multiple times smaller computational cost in the acquisition of BOC signals than conventional FFT-based BOC acquisition technique. As a result, the proposed technique is beneficial for the receivers to make a quick position fix when there are plenty of strong (i.e., line-of-sight) GNSS satellites to be searched.

ACKNOWLEDGMENTS

This work was supported by Electronics and Telecommunication Research Institute (ETRI) (21ZH1100, Study on 3D Communication Technology for Hyper-Connectivity).

AUTHOR CONTRIBUTIONS

Conceptualization, S.K. and B.K.; methodology, J.H., B.K., and S.K.; software, J.H. and B.K.; validation, J.H. and B.K.; formal analysis, J.H. and B.K.; investigation, J.H. and B.K.; resources, J.H. and B.K.; data curation, J.H. and B.K.; writing—original draft preparation, J.H. and B.K.; writing—review and editing, J.H.; visualization, B.K.; supervision, S.K.; project administration, S.K.; funding acquisition, S.K., J.H., and B.K contributed equally to this work.

CONFLICTS OF INTEREST

The authors declare no conflict of interest.

REFERENCES

Akopian, D. 2005, Fast FFT based GPS satellite acquisition methods, IEE Proceedings-Radar, Sonar and Navigation, 152, 277-286. https://doi.org/10.1049/ip-rsn:20045096

Borio, D. 2011, M-sequence and secondary code constraints for GNSS signal acquisition, IEEE Transactions on Aerospace and Electronic Systems, 47, 928-945. https://doi.org/10.1109/TAES.2011.5751235

Borre, K., Akos, D. M., Bertelsen, N., Rinder, P., & Jensen, S. H. 2007, A software-defined GPS and Galileo receiver: a single-frequency approach (Boston: Springer Science & Business Media). https://doi.org/10.1007/978-0-8176-4540-3

Dovis, F., Presti, L. L., Fantino, M., Mulassano, P., & Godet, J. 2008, Comparison between Galileo CBOC Candidates and BOC(1, 1) in terms of detection performance, International Journal of Navigation and Observation, 2008, Article ID 793868. https://doi.org/10.1155/2008/793868

Fishman, P. M. & Betz, J. W. 2000, Predicting performance of direct acquisition for the M-code signal, In Proceedings of the 2000 national technical meeting of the institute of navigation, Anaheim, CA, 26-28 Jan 2000, pp.574-582.

Geiger, B. C., Soudan, M., & Vogel, C. 2010, On the detection probability of parallel code phase search algorithms in GPS receivers, In 21st Annual IEEE International Symposium on Personal, Indoor and Mobile Radio Communications, Istanbul, Turkey, 26-30 Sept 2010, pp.865-870. https://doi.org/10.1109/PIMRC.2010.5672040

Julien, O., Macabiau, C., Cannon, M. E., & Lachapelle, G. 2007, ASPeCT: unambiguous sine-BOC(n, n) acquisition/tracking technique for navigation applications, IEEE Transactions on Aerospace and Electronic Systems, 43, 150-162. https://doi.org/10.1109/TAES.2007.357123

Kaplan, E. D. & Hegarty, C. J. 2006, Understanding GPS: Principles and Applications, 2nd ed. (Boston: Artech House. Inc.)

Kim, B. & Kong, S. H. 2014a, Two-Dimensional Compressed Correlator for Fast Acquisition of BOC(m, n) Signals, IEEE Transactions on Vehicular Technology, 63, 2662-2672. https://doi.org/10.1109/TVT.2013.2293225

Kim, B. & Kong, S. H. 2014b, Design of FFT-based TDCC for GNSS acquisition, IEEE transactions on wireless communications, 13, 2798-2808. https://doi.org/10.1109/TWC.2014.040714.131884

Kong, S. H. 2013, A deterministic compressed GNSS acquisition technique, IEEE Transactions on Vehicular Technology, 62, 511-521. https://doi.org/10.1109/TVT.2012.2220989

Kong, S. H. & Kim, B. 2013, Two-dimensional compressed correlator for fast PN code acquisition, IEEE transactions on wireless communications, 12, 5859-5867. https://doi.org/10.1109/TWC.2013.092313.130407

Li, H., Cui, X., Lu, M., & Feng, Z. 2008, Dual-folding based rapid search method for long PN-code acquisition, IEEE transactions on wireless communications, 7, 5286-5296. https://doi.org/10.1109/T-WC.2008.071130

Margaria, D., Dovis, F., & Mulassano, P. 2008, Galileo AltBOC signal multiresolution acquisition strategy, IEEE Aerospace and Electronic Systems Magazine, 23, 4-10. https://doi.org/10.1109/MAES.2008.4693984

Papoulis, A. & Pillai, S. U. 2002, Probability, random variables, and stochastic processes (Boston: Tata McGraw-Hill Education).

Spangenberg, S. M., Scott, I., McLaughlin, S., Povey, G. J., Cruickshank, D. G., et al. 2000, An FFT-based approach for fast acquisition in spread spectrum communication systems, Wireless Personal Communications, 13, 27-55. https://doi.org/10.1023/A:1008848916834

Viterbi, A. J. 1995, CDMA: principles of spread spectrum communication (Boston: Addison-Wesley Longman Publishing Co., Inc.).

Yang, C. 2001, FFT acquisition of periodic, aperiodic, puncture, and overlaid code sequences in GPS, In Proceedings of the 14th International Technical Meeting of the Satellite Division of The Institute of Navigation (ION GPS 2001), Salt Lake City, UT, 11-14 Sept 2001, pp.137-147.

Yang, C., Vasquez, J., & Chaffee, J. 1999, Fast direct P (Y)-code acquisition using XFAST, In Proceedings of the 12th International Technical Meeting of the Satellite

Division of The Institute of Navigation (ION GPS 1999), Nashville, TN, 14-17 Sept 1999, pp. 317-324.

Ye, Z., Memik, G., & Grosspietsch, J. 2008, Energy detection using estimated noise variance for spectrum sensing in cognitive radio networks, In 2008 IEEE Wireless Communications and Networking Conference, Las Vegas, NV, 31 March-3 April 2008, pp.711-716.

Yi, J., Shufang, Z., Qing, H., & Xiaowen, S. 2008, A new FFT-based acquisition algorithm for GPS signals, In 2008 International Workshop on Education Technology and Training & 2008 International Workshop on Geoscience and Remote Sensing, Shanghai, China, 21-22 Dec 2008, Vol.2, pp.416-419.

Jeong-Hoon Kim is a engineering intern in the CCS Graduate School of Green Transportation of Korea Advanced Institute of Science and Technology (KAIST). His research interests include reinforcement learning, autonomous driving and GNSS receiver singal processing.

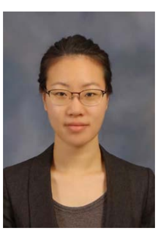

Binhee Kim received the B.S. and M.S. degrees in electrical engineering and the Ph.D. degree from the Korea Advanced Institute of Science and Technology (KAIST), Korea, in 2008, 2010, and 2015, respectively. She is currently working with Korea Aerospace Industries. Her research interests include radar signal processing, and detection and estimation for navigation systems.

Seung-Hyun Kong is an Associate Professor in the CCS Graduate School of Green Transportation of Korea Advanced Institute of Science and Technology (KAIST), where he has been a faculty member since 2010. He received the B.S. degree in Electronics Engineering from Sogang University, Seoul, Korea, in 1992, an M.S. degree in Electrical and Computer Engineering from Polytechnic University (merged to NYU), New York, in 1994, the Ph.D. degree in Aeronautics and Astronautics from Stanford University, Palo Alto, in 2005. From 1997 to 2004 and from 2006 to 2010, he was with companies including Samsung Electronics (Telecommunication Research Center), Korea, and Qualcomm (Corporate R&D Department), San Diego, USA for advanced technology R&D in mobile communication systems, wireless positioning, and assisted GNSS. Since he joined KAIST as a faculty member in 2010, he has been working on various R&D projects in advanced intelligent transportation systems, such as robust GNSS-based navigation for urban environment, deep learning and reinforcement learning algorithms for autonomous vehicles, sensor fusion, and vehicular communication systems (V2X). He has authored more than 100 papers in peer-reviewed journals and conference proceedings and 12 patents, and his research group won the President Award (of Korea) in the 2018 international student autonomous driving competition host by the Korean government. He has served as an associate editor of IEEE T-ITS and IEEE Access, an editor of IET-RSN and the lead guest editor of the IEEE TITS special issue on “ITS empowered by AI technologie” and the IEEE Access special section on “GNSS, Localization, and Navigation Technologies”. He has served as the program chair of IPNT from 2017 to 2019 in Korea and as a program co-chair of IEEE ITSC2019, New Zealand.